BIOCHEMISTRY
including biophysical chemistry & molecular biology

ARTICLE

pubs.acs.org/biochemistry

The Crystal Structure of *Streptococcus pyogenes* Uridine Phosphorylase Reveals a Distinct Subfamily of Nucleoside Phosphorylases

Timothy H. Tran,[†] S. Christoffersen,[‡] Paula W. Allan,[§] William B. Parker,[§] Jure Piškur,[‡] I. Serra,[∥] M. Terreni,[∥] and Steven E. Ealick*[,†]

[†]Department of Chemistry and Chemical Biology, Cornell University, Ithaca, New York 14853-1301, United States

[‡]Department of Cell and Organism Biology, Lund University, Lund, Sweden

[§]Southern Research Institute, Birmingham, Alabama 35205, United States

[∥]Department of Drug Sciences, University of Pavia, via Taramelli 12, 27100 Pavia, Italy

Supporting Information

ABSTRACT: Uridine phosphorylase (UP), a key enzyme in the pyrimidine salvage pathway, catalyzes the reversible phosphorolysis of uridine or 2′-deoxyuridine to uracil and ribose 1-phosphate or 2′-deoxyribose 1-phosphate. This enzyme belongs to the nucleoside phosphorylase I superfamily whose members show diverse specificity for nucleoside substrates. Phylogenetic analysis shows *Streptococcus pyogenes* uridine phosphorylase (SpUP) is found in a distinct branch of the pyrimidine subfamily of nucleoside phosphorylases. To further characterize SpUP, we determined the crystal structure in complex with the products, ribose 1-phosphate and uracil, at 1.8 Å resolution. Like *Escherichia coli* UP (EcUP), the biological unit of SpUP is a hexamer with an α/β monomeric fold. A novel feature of the active site is the presence of His169, which structurally aligns with Arg168 of the EcUP structure. A second active site residue, Lys162, is not present in previously determined UP structures and interacts with O2 of uracil. Biochemical studies of wild-type SpUP showed that its substrate specificity is similar to that of EcUP, while EcUP is ∼7-fold more efficient than SpUP. Biochemical studies of SpUP mutants showed that mutations of His169 reduced activity, while mutation of Lys162 abolished all activity, suggesting that the negative charge in the transition state resides mostly on uracil O2. This is in contrast to EcUP for which transition state stabilization occurs mostly at O4.

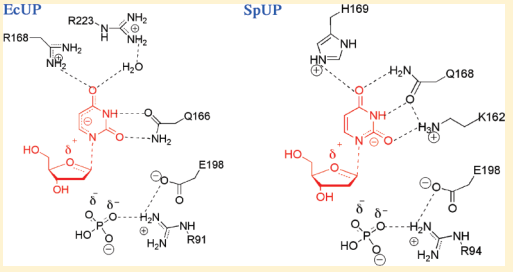

Uridine phosphorylase (UP, EC 2.4.2.3) is a key enzyme in the pyrimidine salvage pathway and is found in most prokaryotes and eukaryotes. The salvage pathway is an alternative to the energetically expensive de novo biosynthetic pathway, which requires six biochemical transformations to make precursors for DNA and RNA biosynthesis.[1] Specifically, UP uses free phosphate to catalyze the reversible phosphorolysis of ribonucleosides or 2′-deoxynucleosides of uracil and their analogues to the corresponding nucleobases and (2′-deoxy)ribose 1-phosphate (R1P). In addition, UP is essential for utilizing nucleosides as a carbon source during pyrimidine catabolism.[2] Several structures of UPs have been reported, and roles of active site residues have been proposed.[3−7] All known UPs belong to the nucleoside phosphorylase I (NP-I) superfamily;[8] however, mammalian UPs are dimers, while bacterial UPs are hexamers comprised of a trimer of dimers. Other NP-I families include purine nucleoside phosphorylase (PNP), methylthioadenosine phosphorylase, adenosine 5′-monophosphate nucleosidase (AMN), and 5′-methylthioadenosine/*S*-adenosylhomocysteine nucleosidase (MTAN).

Nucleoside phosphorylases are also known to inactivate certain pyrimidine and purine nucleoside analogues with potential antitumor properties.[7,9] For example, the pyrimidine analogue 5-fluorouracil is used as a chemotherapeutic agent for the treatment of advanced stage colorectal cancer.[10] However, the nucleoside analogue 5-fluorouridine is cleaved by UP and, consequently, no more effective than 5-fluorouracil itself. Thus, inhibitors of human UP enzymes might enhance the efficacy of certain pyrimidine nucleoside analogues. Mechanisms of inhibition of UPs by analogues have been proposed.[7,11] Despite these studies, the details of the chemical mechanism and the role of active site residues are not as well understood as those of PNP.[12−16] For example, in the presence of the sulfate, which has been used previously as an unreactive mimic of phosphate,[14] some pyrimidine nucleosides cleave to form a ribosyl intermediate and the free base. Interestingly, the proposed ribosyl intermediate exists as a glycal, a phenomenon that has not been observed previously in nucleoside phosphorylases.[6]

The catalytic mechanism of PNPs, which is expected to be similar to that of the UPs, has been extensively explored by enzyme

Received: May 7, 2011
Revised: June 27, 2011
Published: June 27, 2011

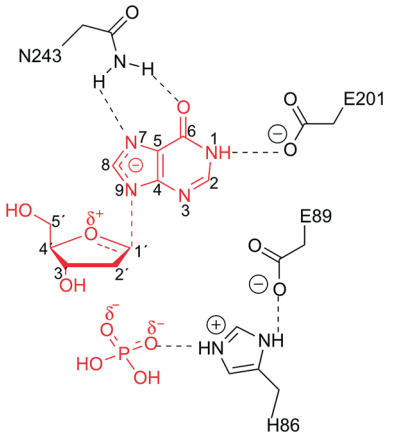

Figure 1. Proposed transition state for PNP from human blood.[12]

kinetics. The deuterium kinetic isotope effect that occurred during the phosphorolytic reaction supports an S_N1 mechanism.[17,18] This mechanism was further validated by studies of the arsenolysis reaction that demonstrated the existence of oxocarbenium ion character during the transition state.[15] The resulting high-energy oxocarbenium ion is stabilized by a continuum of electrostatic interactions among the substrate intermediates and conserved residues in the active site.[12,14] The scheme for the proposed transition state stabilization is shown in Figure 1.

Here we report the X-ray structure of *Streptococcus pyogenes* UP (SpUP) in complex with the products ribose 1-phosphate and uracil (SpUP−R1P−Ura) at 1.8 Å resolution. The three-dimensional structure shows that the overall monomeric fold is similar to that of the NP-I superfamily; however, unlike previously reported UP structures, SpUP lacks the two critical active site arginine residues that are proposed to stabilize the negative charge that accumulates on the pyrimidine ring during formation of the oxocarbenium-like transition state.[3,6] Instead, SpUP utilizes one histidine residue and one lysine residue for this purpose. These residues are conserved within a group of UPs and thus establish a previously unrecognized subfamily. We also report biochemical studies of wild-type and mutant SpUP that aimed to probe substrate specificity, mechanism, and catalytic efficiency. Lys162 was found to be essential through electrostatic interactions with uracil O2. As a result of the differences in active site residues and differences in transition state stabilization, *Escherichia coli* UP (EcUP) is ∼7 times more efficient than SpUP.

MATERIALS AND METHODS

Cloning of Native SpUP. The *up* gene was amplified via polymerase chain reaction (PCR) from *S. pyogenes* (ATCC 12344) genomic DNA using the following primers: upstream primer, 5′-GGG TAG CAT ATG CAA AAT TAT TCA GGT GAA GTC GG-3′ (inserts an *Nde*I site at the start codon of the *up* open reading frame); downstream primer, 5′-CCC TAC TCG AGT TAT TGT GAT TTA TCA TTT TCA ATA AG-3′ (inserts an *Xho*I site after the end of the *up* open reading frame). The purified PCR product was digested with *Nde*I and *Xho*I, purified, and ligated into similarly digested pTHT (a pET-28-derived vector that incorporates a modified six-His tag followed by a TEV protease cleavage site onto the N-terminus of the expressed protein). Kanamycin-resistant colonies were screened for presence of the insert, and a representative plasmid was designated pSpUP.THT. The PCR-derived DNA was sequenced and shown to contain no errors.

Mutagenesis of SpUP. Standard methods were used for DNA manipulations.[19,20] Plasmid DNA was purified with the Fermentas GeneJet Miniprep kit. *E. coli* strain MachI (Invitrogen) was used as a recipient for transformations during plasmid construction and for plasmid propagation and storage.

Site-directed mutagenesis was performed on pSpUP.THT with a standard PCR protocol using *Pfu*Turbo DNA polymerase per the manufacturer's instructions (Invitrogen) and *Dpn*I (New England Biolabs) to digest the methylated parental DNA prior to transformation.

In addition to the forward and reverse primers required to introduce the mutation, a third primer was designed to screen for the presence of the mutation by colony PCR (Table S1 of the Supporting Information).

Expression and Purification of SpUP. The plasmid described above was transformed into *E. coli* expression strain BL21(DE3) cells. An overnight culture of 10 mL was grown in LB medium at 37 °C supplemented with 50 μg/mL kanamycin and then introduced into a 1 L culture containing 50 μg/mL kanamycin. The culture was grown at 37 °C with shaking until an OD_{600} of 0.6 was reached, at which point the temperature was reduced to 15 °C and isopropyl 1-β-D-galactopyranoside was added to a final concentration of 1 mM. Cells were harvested by centrifugation at 7459*g* for 20 min after growing for approximately 16 h. The pellet was stored at −80 °C until it was purified.

The frozen cell pellet was thawed overnight at 4 °C and resuspended in approximately 30 mL of lysis buffer [20 mM Tris (pH 8), 10 mM imidazole, and 300 mM NaCl]. The cell suspension was sonicated and then centrifuged at 47488*g* for 1 h to remove the cellular debris. All the steps after cell lysis were performed at 4 °C. The clarified lysate was loaded onto a pre-equilibrated Ni-NTA gravity column with a volume of 1 mL, after which the column was rinsed with 20 column volumes of lysis buffer. SpUP was then eluted with 10 mL of elution buffer [20 mM Tris (pH 8), 300 mM imidazole, 10% glycerol, and 300 mM NaCl]. The eluted protein was loaded directly onto a size exclusion column (Hiload 26/60 Superdex 200 pg, GE Healthcare) for further purification. The protein fractions from the column were pooled together and, using an Amicon Ultra centrifugal filter, concentrated to 25−30 mg/mL as determined by the method of Bradford.[20] The protein was confirmed to be at least 95% pure by sodium dodecyl sulfate−polyacrylamide gel electrophoresis analysis. The pure protein was buffer exchanged into 20 mM Tris (pH 8), 50 mM NaCl, and 1 mM DTT, flash-frozen in liquid nitrogen, and stored at −80 °C until use.

Crystallization of SpUP with Products. Frozen SpUP was thawed at 4 °C and incubated for 12 h with 8 mM R1P and 8 mM uracil in Tris buffer (pH 8). Cocrystallization trials were initially conducted using the vapor diffusion hanging drop method at 22 °C with sparse matrix screening solutions (Hampton Research, Emerald Biosystems). For each drop, 1 μL of protein solution was combined with an equal volume of well solution. The SpUP−R1P−Ura complex crystallized in 0.1 M sodium citrate (pH 5.2), 18% (w/v) PEG 4000, and 16% 2-propanol. The plate-like crystals took 3−7 days to grow and grew to a maximum size of 0.1 mm × 0.2 mm × 0.45 mm. The crystals belonged to space group *P*1, with a unit cell volume consistent with three complete hexamers per asymmetric unit (Table 1). No additional cryoprotectant was used for crystal freezing.

Table 1. Data Collection and Refinement Statistics of the SpUP−R1P−Ura Complex[a]

beamline	24-ID-C, NE-CAT, APS
wavelength (Å)	0.97849
space group	*P*1
unit cell dimensions	a = 90.0 Å, b = 91.7 Å, c = 169.3 Å, α = 78.5°, β = 82.3°, γ = 60.1°
no. of chains per asymmetric unit	18
resolution (Å)	50−1.8
total no. of reflections	793731 (30451)
no. of unique reflections	404352 (16027)
redundancy	2.0 (1.9)
R_{merge} (%)[b]	4.9 (20.5)
$I/\sigma(I)$	19.3 (4.1)
no. of reflections in the working set	383726
completeness (%)	94.6 (74.7)
R_{work}/R_{free}[c] (%)	17.7/20.3
no. of protein atoms	33711
no. of ligand atoms	396
no. of water atoms	2979
average *B* factor for protein (Å^2)	13.3
average *B* factor for water (Å^2)	23.6
average *B* factor for ligand (Å^2)	17.1
rmsd for bonds (Å)	0.005
rmsd for angles (deg)	1.283

[a] Values in parentheses are for the highest-resolution shell. [b] $R_{merge} = \Sigma\Sigma_i|I_i - \langle I\rangle|/\Sigma\langle I\rangle$, where $\langle I\rangle$ is the mean intensity of N reflections with intensities I_i and common indices h,k,l. [c] $R_{work} = \Sigma_{hkl}||F_o| - k|F_c||/\Sigma_{hkl}|F_o|$, where F_o and F_c are observed and calculated structure factors, respectively, calculated over all reflections used in the refinement. R_{free} is similar to R_{work} but calculated over a subset of reflections (5%) excluded from all stages of refinement.

Data Collection and Processing. Data for SpUP−R1P−Ura were collected at 100 K using NE-CAT beamline 24-ID-C at the Advanced Photon Source (APS) at Argonne National Laboratory using a Quantum 315 X-ray detector (Area Detector Systems Corp.). The data were collected at a wavelength of 0.9785 Å over 360° using a 0.5° oscillation range. All data were indexed, integrated, and scaled using the HKL2000 program suite.[21] The data collection statistics are listed in Table 1.

Structure Determination. The SpUP structure was determined by molecular replacement with EcUP [Protein Data Bank (PDB) entry 1K3F][5,22] as the search model, using MolRep in the CCP4 program suite.[23] CHAINSAW in the CCP4 suite was used to prune the side chains of the search model to the last common atom. The relatively large unit cell and predicted solvent content suggested three complete hexamers per asymmetric unit. The three hexamers showed pseudotranslational symmetry except that one hexamer was significantly tilted with respect to the other two. After one round of tight rigid body refinement followed by a round of restrained refinement in Refmac5 of the CCP4 program suites, R_{factor} and R_{free} decreased to 32.4 and 34.7%, respectively. In subsequent rounds of refinement, the restraints were gradually relaxed. Most of the side chains were built during these rounds of refinement. Further rounds of refinement were performed in CNS[24] starting with rigid body refinement, simulated annealing, and finally *B* factor refinement. Difference Fourier maps ($F_o - F_c$ and $2F_o - F_c$) and composite omit maps were calculated from models after each round of refinement. Manual model building was done using Coot[25] and the noncrystallographic symmetry (NCS)-averaged composite omit map to minimize model bias. Water molecules were added after the convergence of R_{factor} and R_{free}. The ligands were modeled into all 18 active sites of SpUP. The ligands were generated using PRODRG.[26] The geometry of SpUP was validated using PROCHECK.[27] The final R_{factor} and R_{free} converged to 17.7 and 20.3%, respectively. The complete refinement statistics are listed in Table 1.

Determination of Substrate Specificity. In 1 mL total reaction volumes containing 100 mM HEPES and 50 mM phosphate buffer (K_2HPO_4) with a final pH of 7.4, an appropriate amount of SpUP was incubated with 500 μM substrate. Samples (150 μL) were removed from the reaction mixture after incubation for 0, 0.25, 0.5, 1, and 2 h and immediately mixed with 150 μL of water, and the reactions were quenched by boiling. The precipitated protein was removed by filtration using a 0.2 μm syringe filter, and the sample was injected onto a 5 μm BDS Hypersil C-18 column (150 mm × 4.6 mm) (Keystone Scientific Inc., State College, PA). The mobile phase was a 12.5 mM ammonium dihydrogen phosphate buffer (pH 4.5) containing 1.25% acetonitrile (flow rate of 1 mL/min). Substrates and products were detected by their absorbance at 260 nm as they eluted from the column.

Steady State Kinetic Measurements for SpUP and EcUP. All uridine phosphorolysis reactions were conducted in a 500 μL total volume containing 50 mM phosphate buffer (K_2HPO_4) and 50 mM HEPES with a final pH of 7.5. In the reaction buffer described above containing a known amount of uridine substrate, the reaction was initiated by the addition of SpUP, H169A, K162A, or EcUP to a final concentration of 41, 425, 2000, or 7 nM, respectively. The concentrations are calculated for the monomers. At these concentrations, the enzymes were completely quenched by the addition of 10 μL of 10 M NaOH, which allowed the appearance of the absorbance peak of the uracil product to be monitored at 290 nm.[28] The initial rate for each uridine concentration was measured when the reaction had proceeded approximately 10% toward completion. All the initial rates were then plotted and fitted to the Michaelis−Menten equation using Kaleidagraph (Synergy Software). In two duplicate sets of experiments, the reaction was quenched with acetic acid and heat (100 °C) before NaOH was added to ensure that the measurements were consistent.

Figure Preparation. Figures were prepared using PyMOL[29] and ChemBioDraw (CambridgeSoft).

RESULTS

Quaternary Structure of SpUP. As expected from the relatively high level of sequence identity with EcUP (40%) and recent classification,[8] the biological unit of SpUP is a hexamer with 32 symmetry (Figure 2a). The toroidal hexamer has a diameter of approximately 100 Å and a thickness of 40 Å. The hexamer of SpUP also has a central channel with a diameter of 18 Å. The oligomeric state was also confirmed by the size exclusion chromatography data, which estimated the molecular mass of the SpUP oligomer to be approximately 167 kDa. While each protomer contains an active site, the active site is located at a dimer interface and contains two residues, His13 and Arg51, from the adjacent monomer. Thus, the minimal functional unit is a dimer. The distance between two active sites, which are

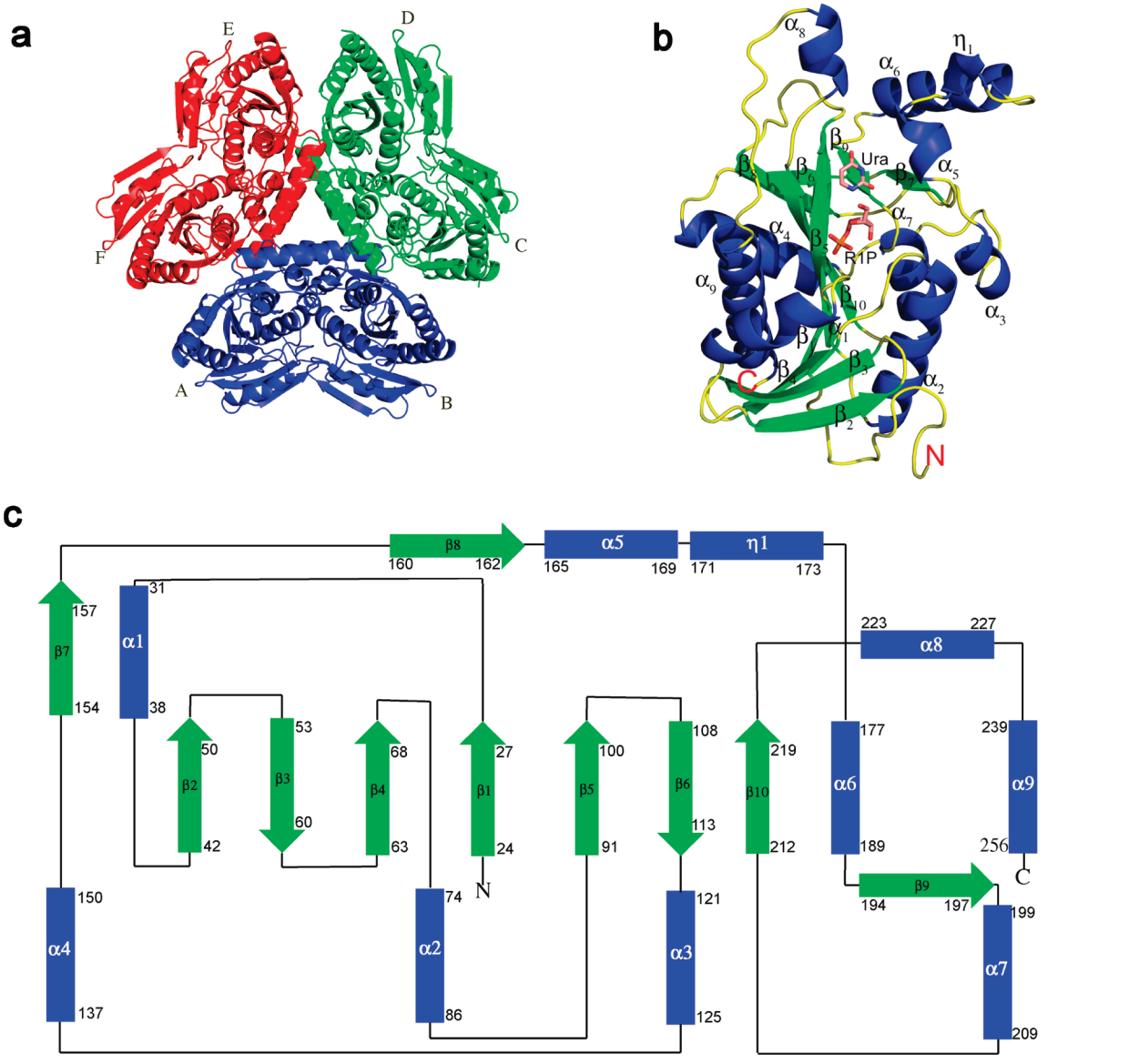

Figure 2. Structures of SpUP. (a) Hexameric quaternary structure of SpUP color-coded to emphasize the 32 point symmetry or a trimer of dimers. Six subunits are labeled A−F. (b) SpUP protomer with the bound products, R1P and Ura, shown in the active site. The helices are colored blue, the strands green, and the loops yellow. The N-terminus and the C-terminus are also indicated with letters N and C, respectively. (c) Topology diagram of the SpUP protomer. The colors of the helices and strands are the same as in Figure 1b, except the loops are depicted as black lines. The first and last residues of each secondary structure are indicated by numbers.

located on opposite faces of the hexamer, is ∼21 Å. In the SpUP−R1P−Ura crystal structure, three hexamers are found in the asymmetric unit complex.

Structure of the SpUP Protomer. The SpUP protomer shown in Figure 2b adopts an α/β-fold. The core contains a mixed eight-stranded β-sheet with a sharp twist in a $\beta_2\uparrow\beta_3\downarrow\beta_4\uparrow\beta_1\uparrow\beta_5\uparrow\beta_{10}\uparrow\beta_8\downarrow\beta_6\downarrow$ orientation. The topology diagram for SpUP is shown in Figure 2c. The β-sheet is flanked by six α-helices, with α_1, α_4, and α_9 on one side and α_2, α_3, and α_7 on the other. β_2, β_5, and β_{10} are longer than the rest of the β-strands, containing 9, 10, and 8 residues, respectively. α-Helices α_5, α_6, and α_8 as well as a 3_{10}-helix (η_1) are clustered on one side of the active site. Four α-helices, α_2, α_4, α_6, and α_9, are much longer than other helices. Helix α_9, capping the C-terminus, is the longest (17 residues), whereas helices α_2, α_4, and α_6 contain 11, 13, and 13 residues, respectively. The loop between α_8 and α_9, consisting of residues 234−238, generally has weak electron density and high *B* factors.

SpUP Active Site. Figure 3 illustrates the active site for the SpUP−R1P−Ura complex. The most significant feature of the phosphate binding site is the presence of three highly conserved arginine residues, Arg33, Arg51*, and Arg94 (the asterisk denotes a residue from a neighboring monomer). The three arginine residues position the phosphate moiety of R1P with a strong ionic network. Two other conserved residues also form hydrogen bonds to the phosphate group: Gly29 via the amide nitrogen atom and Thr97 via its side chain. In addition, the oxygen atom of the phosphate ion closest to the ribose also forms a hydrogen bond to O3′ of the sugar moiety.

Figure 3b shows the ribose binding site. The 2′- and 3′-hydroxyl groups form a pair of hydrogen bonds with Glu198.

dx.doi.org/10.1021/bi200707z |*Biochemistry* 2011, 50, 6549–6558

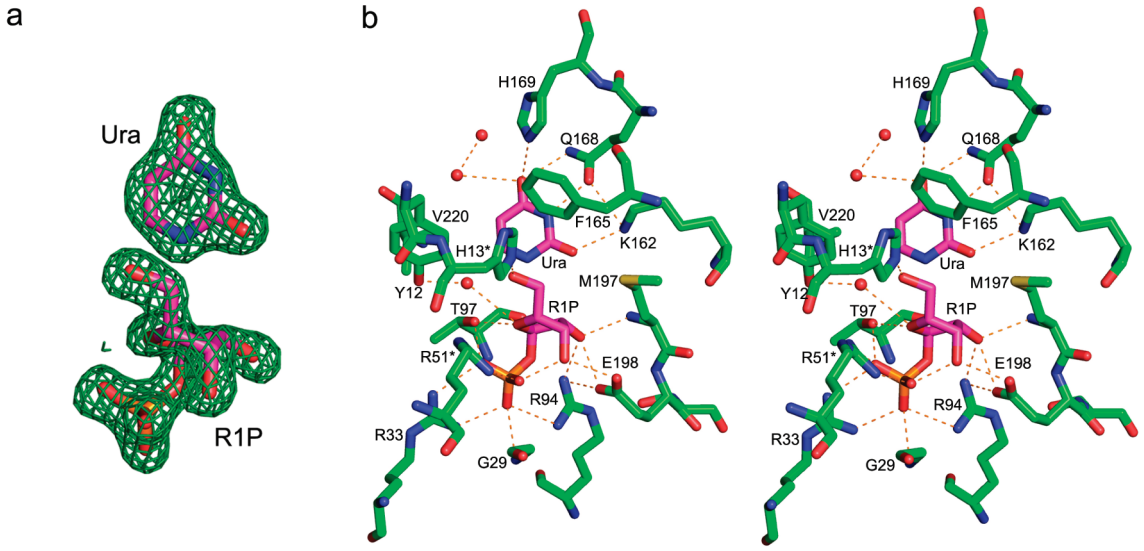

Figure 3. Active site of SpUP. (a) Electron density for uracil and R1P. The NCS-averaged $F_o - F_c$ density was calculated with phases from the refined model after the ligands were removed. The map is contoured at 3.0σ. (b) Stereoview of the active site containing R1P and Ura. The red spheres represent water molecules. Hydrogen bonds are represented with dashed lines.

Table 2. SpUP Substrate Specificity

substrate	cleavage activity (nmol mg^{-1} h^{-1})	substrate	cleavage activity (nmol mg^{-1} h^{-1})
uridine	485000	deoxycytidine	<10000
deoxyuridine	673000	adenosine	<10000
thymidine	352000	guanosine	<10000
cytidine	<10000	inosine	<10000

The C2′-hydroxyl forms a second hydrogen bond with Arg94. His13*, which is conserved in all UPs, forms a hydrogen bond to the hydroxyl group of C5′. Thr97 forms a weak hydrogen bond with O4′ of the ribose ring. The sulfur atom of the highly conserved Met197 interacts with the hydrophobic face of the ribose and could be involved in positioning the substrate within the active site.[12] In addition, the main chain nitrogen atom of Met197 forms a hydrogen bond to the 2′-hydroxyl group. This methionine residue is conserved throughout the entire NP-I family. A conserved water molecule also forms a hydrogen bond to the O4′ atom of the sugar group.

While the phosphate and ribose binding sites are both similar to those of EcUP,[3] the uracil binding site shows significant differences. Nδ of His169 is located approximately 3 Å from the O4 atom of the uracil base; however, the N−H···O angle is 120°, suggesting a weak hydrogen bond. Gln168 is strictly conserved among all the known UP structures and makes hydrogen bonds with the N3 and O4 atoms of the uracil base. Lys162 is coplanar with the uracil and forms hydrogen bonds to O2 as well as to Gln168. Phe165 forms a herringbone interaction with the aromatic ring of the uracil. Val220 interacts with the hydrophobic portion of the uracil ring.

Substrate Specificity. Because of the variation in the active site residues compared to EcUP, we tested the ability of SpUP to cleave other purine and pyrimidine nucleosides. SpUP cleaves uridine, deoxyuridine, and thymidine, but not cytidine, deoxycytidine, adenosine, inosine, or guanosine. Results are listed in Table 2.

Uridine Phosphorolysis Assay. Using the crystal structure, several SpUP mutants were designed to probe the roles of active site residues in the base binding region. Lys162 was mutated to alanine, and His169 was mutated to alanine, asparagine, and aspartate. In addition, Val220 was mutated to aspartate and glutamate to determine if the enzyme could accommodate a purine base in the presence of these polar, charged groups. Mutation of Lys162 abolished activity, while the other mutations showed various levels of reduction of activity. The results for all SpUP mutants are listed in Table 3.

Steady State Kinetic Measurements for SpUP and EcUP. The UV spectra of uridine and uracil are very similar. Therefore, to spectrophotometrically monitor the formation of the uracil product, an aliquot of 10 μL of 10 M NaOH (0.2 M) was added to the reaction mixture. This amount of base was sufficient to quench the reaction and to deprotonate the free uracil, and thus to change the aromaticity of the uracil ring. This gave rise to a large absorption peak at 290 nm for the free uracil.[28] The same amount of base has no effect on uridine. The robustness of this assay was confirmed by duplicate experiments, in which the reaction was quenched with acetic acid or heat (100 °C) before NaOH was added. Table 4 shows the resulting steady state parameters for SpUP and EcUP.

DISCUSSION

Overall Structure of SpUP. The biological unit of SpUP is a hexamer, as is the case for other prokaryotic UPs (Figure 2a).[3,30] The asymmetric unit of the SpUP−R1P−Ura complex contains three hexamers. While two of the hexamers exhibit good translational pseudosymmetry, with a center−center separation of ~55 Å, the 3-fold axis of the third hexamer is tilted 37° with respect to the other two, resulting in space group *P*1 (Table 1). The SpUP protomers superimpose well on the EcUP protomer, especially in the active site, with a root-mean-square deviation of the Cα atoms ranging from 0.99 to 1.05 Å (Figure 4). SpUP adopts the canonical α/β-fold of the NP-I superfamily.[8] Residues 170−182, including the 3_{10}-helix (η_1) and part of α_6, comprise

dx.doi.org/10.1021/bi200707z |*Biochemistry* 2011, 50, 6549–6558

Table 3. Uridine Phosphorolysis Assay Results for SpUP and Its Mutants

SpUP	uridine cleavage activity (nmol mg^{-1} h^{-1})	SpUP	uridine cleavage activity (nmol mg^{-1} h^{-1})
wild-type	1500000	H169N	42000
K162A	<20	V220D	550
H169A	112000	V220E	3400
H169D	9000		

Table 4. Steady State Kinetic Parameters for SpUP and EcUP[a]

enzyme	k_{cat} (s^{-1})	K_m (mM)	k_{cat}/K_m (mM^{-1} s^{-1})
SpUP	15 ± 3	0.158 ± 0.025	95 ± 24
EcUP	23 ± 1	0.036 ± 0.004	639 ± 76
SpUP H169A	1.7 ± 0.2	0.171 ± 0.005	9.9 ± 1
SpUP K162A[b]	–	–	not applicable

[a] The concentration of uridine was varied, and the production of uracil was monitored. [b] No activity was observed at the level of detection of the assay.

an insertion characteristic of UPs,[3] which allows pyrimidine nucleosides such as uridine and thymidine to bind to the active site while excluding purine nucleosides. The primary sequence alignment demonstrating this insertion is shown in Figure 5. As shown in the alignment, SpUP has two fewer residues in this specificity region compared to EcUP; however, this insertion is absent in *E. coli* purine nucleoside phosphorylase (EcPNP) and thus allows EcPNP to accommodate purine bases.

Comparison of SpUP with Other NP-I Enzymes. SpUP was compared with related but divergent NP-I enzymes, including EcPNP (PDB entry 1PR0),[31] *E. coli* AMN (EcAMN, PDB entry 1T8S),[32] and *E. coli* MTAN (EcMTAN, PDB entry 1NC1).[33] Examination of the biological unit of SpUP and those of the selected NP-I enzymes reveals that although these enzymes have different substrate specificities and use different nucleophiles for the cleavage reactions, they all share the same monomeric fold. Three of the enzymes are hexamers, while EcMTAN is a dimer.

The secondary structure of these enzymes around the active sites and the geometry of substrate binding are highly conserved among these enzymes. Several critical active site residues are conserved among the four structures: (1) a histidine residue from a neighboring protomer that forms a hydrogen bond with the ribose 5′-hydroxyl group, (2) an aromatic residue that stacks against the nucleobase, (3) a strictly conserved glutamate residue that forms hydrogen bonds with both the 2′- and 3′-hydroxyl groups of the ribose, and (4) a methionine residue that packs against the hydrophobic β-face of the ribose to position it in the active site. Residues in the phosphate binding site of SpUP and EcPNP (as well as EcUP) are also highly conserved but are different from those in human PNP[34] or the nucleosidase,[32] which utilize water as the nucleophile.

Substrate Specificity for SpUP. Enzymes in the NP-I family are generally specific for either a purine nucleoside or pyrimidine nucleoside, and the nucleophile can be either phosphate or water. An exception is the PNP from *Plasmodium falciparum*, which can also cleave uridine, but at much lower levels.[35] Nucleoside specificity within the NP-I family results from the size of the base binding site and complementarity of hydrogen bonding at the periphery of the purine or pyrimidine base. Two active site residues, Lys162 and His169, that were not previously observed in the active sites of NP-I family members and a slight variation in the size of the loop that normally discriminates between purine and pyrimidine nucleosides led us to determine the SpUP substrate specificity. The results listed in Table 4 indicate that the preferred substrate specificity is as follows: deoxyuridine (138%) > uridine (100%) > thymidine (73%). The level of cleavage of cytidine, deoxcytidine, adenosine, inosine, or guanosine was below detectable levels.

Comparison of the Steady State Kinetic Parameters for SpUP and EcUP. The discovery of SpUP, which catalyzes the same reaction as EcUP but uses different active site residues compared to EcUP, led us to determine if the two UPs had different catalytic efficiencies. Steady state kinetics showed that the turnover number (k_{cat}) of SpUP equals 15 s^{-1}, with an apparent substrate binding affinity (K_m) of 0.158 mM, which give an overall catalytic efficiency of 95 mM^{-1} s^{-1} (Table 4). The corresponding k_{cat} value for EcUP is 23 s^{-1}, which is slightly higher than that of SpUP, whereas its K_m value (0.036 mM) is 4-fold lower than that of SpUP, giving a catalytic efficiency of 639 mM^{-1} s^{-1} for EcUP. The previously reported value for the K_m of EcUP determined at 25 °C and pH 7.4 is 0.091 mM,[36] which is more than 2-fold higher than the value measured under similar conditions in our base-quench assay. Thus, the catalytic efficiency of EcUP is nearly 7 times higher than that of SpUP.

Substrate Specificity and Mechanistic Implications. Mutation of active site residues provided insight into the roles of key residues (Table 3). The most striking result was the complete loss of activity for the K162A mutant. The enzyme still maintains low but detectable levels of activity with the H169A (8%), H169N (3%), and H169D (1%) mutants. In the SpUP complex, Lys162 forms a hydrogen bond to O2 of uracil, suggesting that this is the major site for accumulation of negative charge. His169 is near O4, but the hydrogen bonding geometry is not optimal, although it is possible that tilting of the base in the substrate complex might provide a more favorable geometry. In the H169N mutant, hydrogen bonding to O4 might still be possible and, in the H169A mutant, a water molecule might occupy the vacant side chain space and provide a hydrogen bond. Assuming that the side chain in the H169D mutant is mostly ionized, hydrogen bonding is not favored. These results suggest that a small amount of negative charge accumulates on O4 during catalysis; however, most of the negative charge would be on O2 and stabilized by Lys162. Val220 was mutated to aspartate and glutamate because acidic side chains are sometimes found in this position in the purine nucleoside phosphorylases; however, these mutants had very low activity. In addition, the active site loop insertion is consistent with exclusion of purine nucleosides.

While enzymes in the NP-I family are generally specific for either a purine nucleoside or a pyrimidine nucleoside and the nucleophile can be either phosphate or water, all family members are believed to function through a high-energy oxycarbenium ion intermediate and require acidic residues or strong hydrogen bond donors to stabilize the negative charge that accumulates on the purine or pyrimidine nucleobase during glycosidic bond cleavage. Various NP-I family members have evolved to promote glycosidic bond cleavage (Figure 6). In the case of purine nucleosides, activation of the leaving group is usually provided by a hydrogen bond to the purine N7 atom using either an asparagine or protonated aspartic acid residue. SpUP and EcUP both catalyze the phosphorolytic cleavage of the glycosidic bond

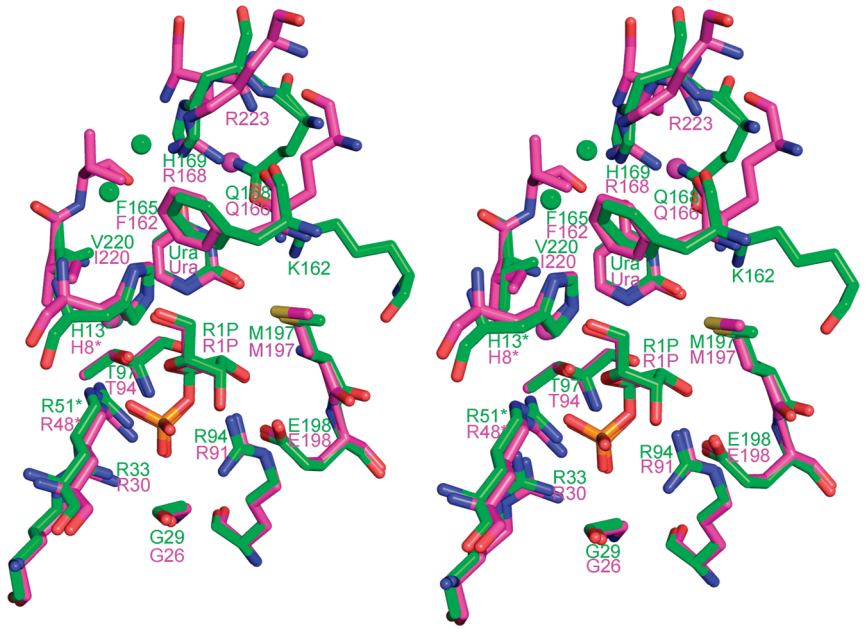

Figure 4. Superposition of the active sites of SpUP (green) and EcUP (magenta) in stereo. The spheres are water molecules found in the active site.

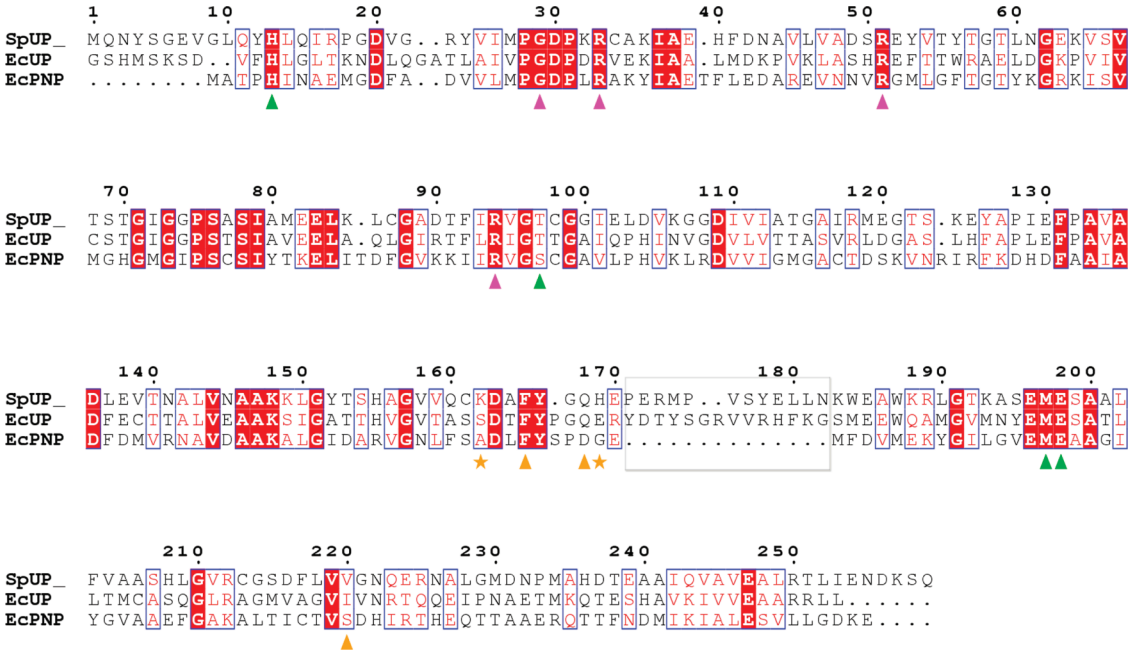

Figure 5. Insertion region (gray box) of SpUP revealed by the alignment of SpUP with EcUP and EcPNP. Magenta, green, and orange triangles denote conserved residues in the phosphate-binding site, ribose-binding site, and uracil-binding site of SpUP, respectively. The residues marked with an asterisk are the two novel residues found in the uracil-binding site of SpUP.

of uridine and related nucleosides; however, differences in active site residues suggest different mechanisms for activation of the leaving group and stabilization of the negative charge resulting from formation of the oxycarbenium ion (Figure 7). EcUP and most other UPs utilize two arginine residues (Arg168 and Arg223) to stabilize negative charge and activate the leaving group.[3] Arg168 forms hydrogen bonds directly to O4, while Arg223 forms hydrogen bonds to O4 through a tightly bound water molecule. Conserved Gln166 donates a hydrogen bond to O2 and accepts a hydrogen bond from N3. In SpUP, Arg168 is replaced with His169 but Arg223 is completely absent. Instead, Gln166 is replaced with Gln168, which shifts to accept a hydrogen bond from N3 and donate a hydrogen bond to O4. The shift of Gln168 makes room for Lys162, which donates a hydrogen bond to O2. Our studies suggest that this hydrogen bond is the primary source of charge stabilization and leaving group activation.

Implications for Evolution of the UPs. Comparison of the active sites of SpUP and EcUP suggests that the two enzymes have similar transition states; however, SpUP utilizes different

dx.doi.org/10.1021/bi200707z |*Biochemistry* 2011, 50, 6549–6558

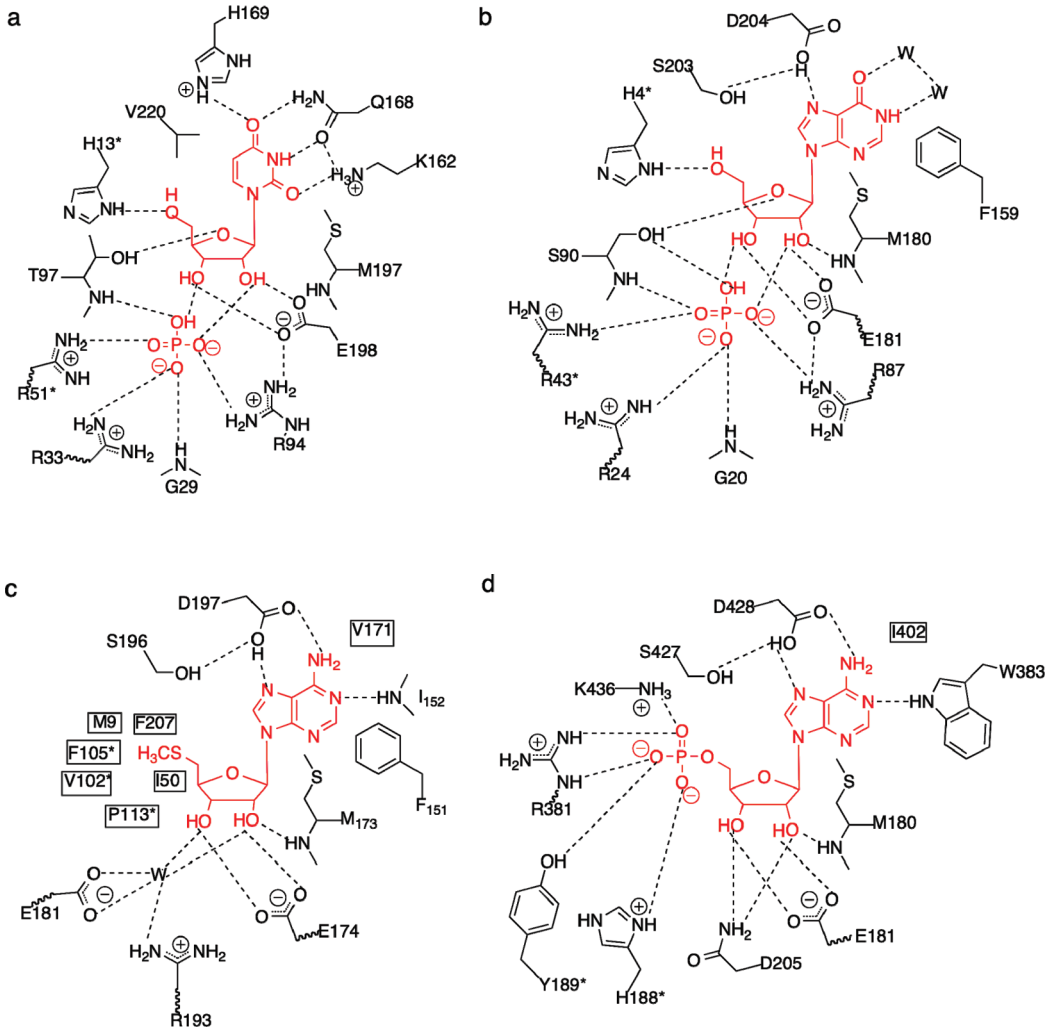

Figure 6. Active sites of SpUP with uridine and phosphate manually positioned in the active site (a), the EcPNP−inosine−PO_4 complex (b), the EcMTAN−5′-methylthiotubercidin complex (c), and the EcAMN−formycin 5′-monophosphate complex (d).[14,31−33] W stands for water. Residues marked with an asterisk come from an adjacent monomer.

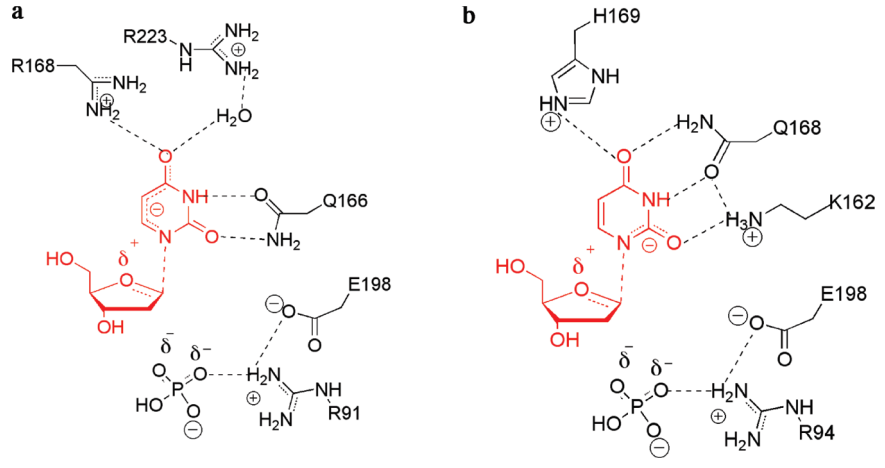

Figure 7. Transition state stabilization of high-energy intermediates of the phosphorolysis reaction in EcUP (a) and SpUP (b) by a continuum of electrostatic and hydrogen bond interactions as illustrated by the dotted line.

residues to stabilize the negative charge on the base. To determine the distribution of the two subfamilies, a multiple-sequence alignment of SpUP and EcUP with sequences found using a BLAST search against the nonredundant database was performed

using ClustalW.[37] After removal of partial sequences and sequences that are more than 95% identical in sequence with an included sequence, 106 UP sequences remained. Among these sequences, 49 UPs were found to contain conserved lysine and histidine residues equivalent to Lys162 and His169 of SpUP. None of these UPs have residues equivalent to Arg168 or Arg223 in EcUP. On the other hand, 57 of the sequences possess the two arginine residues equivalent to Arg168 or Arg223 found in EcUP, but none of these have the residues equivalent to Lys162 and His169 in SpUP. These 106 sequences, including SpUP and EcUP, were placed on a phylogenetic tree using the same ClustalW server. All the SpUP-like species are found in one cluster (Figure S1 of the Supporting Information), while the EcUP-like species are found in a different cluster (Figure S2 of the Supporting Information). Further examination of the alignment indicates that most of the SpUP-like species are from Gram-positive bacteria, while most of the EcUP-like species are from Gram-negative bacteria. Two exceptions are the *Thermococcus* and *Fusobacteria* species, which fall in the SpUP-like branch.

Interestingly, while UP orthologs are found in both prokaryotes and eukaryotes, no UP othologs were found in archaebacteria. Further examination of available archaebacterial genomes revealed species lacking UP orthologs contained pyrimidine nucleoside phosphorylase (PyNP), which is a member of the nucleoside phosphorylase II superfamily.[38] PyNP is structurally homologous to thymidine phosphorylase; however, the former accepts both uridine and thymidine as substrates, while the latter is found in most prokaryotes and eukaryotes and is highly specific for thymidine.[8]

Our results show clear evidence of evolution of two separate UP subfamilies. Both EcUP and SpUP have similar structures and similar substrate specificities; however, there are critical differences in active site residues, and EcUP is nearly 7 times more efficient than SpUP. The improved catalytic efficiency of EcUP compared to SpUP may provide a competitive advantage for pyrimidine metabolism; however, evolution of two distinct UP subfamilies may result in competitive advantages yet to be discovered.

■ ASSOCIATED CONTENT

Supporting Information. Primers used in site-directed mutagenesis (Table S1) and phylogenetic trees showing the relationship of orthologs of SpUp (Figure S1) and EcUP (Figure S2). This material is available free of charge via the Internet at http://pubs.acs.org.

Accession Codes

The coordinates of the SpUP−R1P−Ura complex have been deposited in the Protein Data Bank as entry 3QPB.

■ AUTHOR INFORMATION

Corresponding Author

*Department of Chemistry and Chemical Biology, Cornell University, Ithaca, NY 14853. Telephone: (607) 255-7961. Fax: (607) 255-1227. E-mail: see3@cornell.edu.

Funding Sources

This work was supported by National Institutes of Health Grant GM73220. J.P. thanks Cancerfonden (Sweden) for the funding support.

■ ACKNOWLEDGMENT

The molecular cloning was provided by Cynthia Kinsland at the Cornell University Protein Production Facility. We are grateful to the staff scientists at the Northeastern Collaborative Access Team beamlines of the Advanced Photon Source for their help with the data collection. Finally, we thank Leslie Kinsland for her assistance during manuscript preparation. This work is based upon research conducted at the Advanced Photon Source on the Northeastern Collaborative Access Team beamlines, which are supported by Grant RR-15301 from the National Center for Research Resources at the National Institutes of Health. Use of the Advanced Photon Source is supported by the U.S. Department of Energy, Office of Basic Energy Sciences, under Contract DE-AC02-06CH11357.

■ ABBREVIATIONS

UP, uridine phosphorylase; PNP, purine nucleoside phosphorylase; SpUP, *S. pyogenes* uridine phosphorylase; EcUP, *E. coli* uridine phosphorylase; EcPNP, *E. coli* purine nucleoside phosphorylase; EcAMN, *E. coli* adenosine 5′-monophosphate nucleosidase; EcMTAN, *E. coli* 5′-methylthioadenosine/*S*-adenosylhomocysteine nucleosidase; bPNP, bovine purine nucleoside phosphorylase; APS, Advanced Photon Source; NP-I, nucleoside phosphorylase I; Ura, uracil; R1P, ribose 1-phosphate; NCS, noncrystallographic symmetry; rmsd, root-mean-square deviation.

■ REFERENCES

(1) Zhang, Y., Morar, M., and Ealick, S. E. (2008) Structural biology of the purine biosynthetic pathway. *Cell. Mol. Life Sci. 65*, 3699–3724.

(2) Leer, J. C., Hammer-Jespersen, K., and Schwartz, M. (1977) Uridine phosphorylase from *Escherichia coli*. Physical and chemical characterization. *Eur. J. Biochem. 75*, 217–224.

(3) Caradoc-Davies, T. T., Cutfield, S. M., Lamont, I. L., and Cutfield, J. F. (2004) Crystal structures of *Escherichia coli* uridine phosphorylase in two native and three complexed forms reveal basis of substrate specificity, induced conformational changes and influence of potassium. *J. Mol. Biol. 337*, 337–354.

(4) Lashkov, A. A., Zhukhlistova, N. E., Gabdoulkhakov, A. H., Shtil, A. A., Efremov, R. G., Betzel, C., and Mikhailov, A. M. (2010) The X-ray structure of *Salmonella typhimurium* uridine nucleoside phosphorylase complexed with 2,2′-anhydrouridine, phosphate and potassium ions at 1.86 Å resolution. *Acta Crystallogr. D66*, 51–60.

(5) Morgunova, E., Mikhailov, A. M., Popov, A. N., Blagova, E. V., Smirnova, E. A., Vainshtein, B. K., Mao, C., Armstrong, Sh. R., Ealick, S. E., and Komissarov, A. A. et al. (1995) et al. Atomic structure at 2.5 Å resolution of uridine phosphorylase from *E. coli* as refined in the monoclinic crystal lattice. *FEBS Lett. 367*, 183–187.

(6) Paul, D., O'Leary, S. E., Rajashankar, K., Bu, W., Toms, A., Settembre, E. C., Sanders, J. M., Begley, T. P., and Ealick, S. E. (2010) Glycal formation in crystals of uridine phosphorylase. *Biochemistry 49*, 3499–3509.

(7) Roosild, T. P., Castronovo, S., Fabbiani, M., and Pizzorno, G. (2009) Implications of the structure of human uridine phosphorylase 1 on the development of novel inhibitors for improving the therapeutic window of fluoropyrimidine chemotherapy. *BMC Struct. Biol. 9*, 14.

(8) Pugmire, M. J., and Ealick, S. E. (2002) Structural analyses reveal two distinct families of nucleoside phosphorylases. *Biochem. J. 361*, 1–25.

(9) Renck, D., Ducati, R. G., Palma, M. S., Santos, D. S., and Basso, L. A. (2010) The kinetic mechanism of human uridine phosphorylase 1: Towards the development of enzyme inhibitors for cancer chemotherapy. *Arch. Biochem. Biophys. 497*, 35–42.

(10) Longley, D. B., Harkin, D. P., and Johnston, P. G. (2003) 5-Fluorouracil: Mechanisms of action and clinical strategies. *Nat. Rev. Cancer 3*, 330–338.

(11) Bu, W., Settembre, E. C., el Kouni, M. H., and Ealick, S. E. (2005) Structural basis for inhibition of *Escherichia coli* uridine phosphorylase by 5-substituted acyclouridines. *Acta Crystallogr. D61*, 863–872.

(12) Erion, M. D., Takabayashi, K., Smith, H. B., Kessi, J., Wagner, S., Honger, S., Shames, S. L., and Ealick, S. E. (1997) Purine nucleoside phosphorylase. 1. Structure-function studies. *Biochemistry 36*, 11725–11734.

(13) Erion, M. D., Stoeckler, J. D., Guida, W. C., Walter, R. L., and Ealick, S. E. (1997) Purine nucleoside phosphorylase. 2. Catalytic mechanism. *Biochemistry 36*, 11735–11748.

(14) Federov, A., Shi, W., Kicska, G., Tyler, P. C., Furneaux, R. H., Hanson, J. C., Gainsford, G. J., Larese, J. Z., Schramm, V. L., and Almo, S. C. (2001) Transition State Structure of Purine Nucleoside Phosphorylase and Principles of Atomic Motion in Enzymatic Catalysis. *Biochemistry 40*, 853–860.

(15) Kline, P. C., and Schramm, V. L. (1993) Purine nucleoside phosphorylase. Catalytic mechanism and transition-state analysis of the arsenolysis reaction. *Biochemistry 32*, 13212–13219.

(16) Li, L., Luo, M., Ghanem, M., Taylor, E. A., and Schramm, V. L. (2008) Second-sphere amino acids contribute to transition-state structure in bovine purine nucleoside phosphorylase. *Biochemistry 47*, 2577–2583.

(17) Lehikoinen, P. K., Sinnott, M. L., and Krenitsky, T. A. (1989) Investigation of α-deuterium kinetic isotope effects on the purine nucleoside phosphorylase reaction by the equilibrium-perturbation technique. *Biochem. J. 257*, 355–359.

(18) Stein, R. L., and Cordes, E. H. (1981) Kinetic α-deuterium isotope effects for *Escherichia coli* purine nucleoside phosphorylase-catalyzed phosphorolysis of adenosine and inosine. *J. Biol. Chem. 256*, 767–772.

(19) Ausubel, F. M., and Brent, F. (1987) *Current Protocols in Molecular Biology*, John Wiley and Sons, New York.

(20) Sambrook, J., Fritsch, E. F., and Maniatis, T. (1989) *Molecular Cloning: A Laboratory Manual*, Vol. 3, Cold Spring Harbor Laboratory Press, Plainview, NY.

(21) Otwinowski, Z., and Minor, W. (1997) Processing of X-ray diffraction data collected in oscillation mode. *Methods Enzymol. 276*, 307–326.

(22) Berman, H. M., Westbrook, J., Feng, Z., Gilliland, G., Bhat, T. N., Weissig, H., Shindyalov, I. N., and Bourne, P. E. (2000) The Protein Data Bank. *Nucleic Acids Res. 28*, 235–242.

(23) Collaborative Computational Project-Number 4. (1994) The CCP-4 suite: Programs for protein crystallography. *Acta Crystallogr. D50*, 760–763.

(24) Brünger, A. T., Adams, P. D., Clore, G. M., DeLano, W. L., Gros, P., Grosse-Kunstleve, R. W., Jiang, J. S., Kuszewski, J., Nilges, M., Pannu, N. S., Read, R. J., Rice, L. M., Simonson, T., and Warren, G. L. (1998) Crystallography & NMR system: A new software suite for macromolecular structure determination. *Acta Crystallogr. D54*, 905–921.

(25) Emsley, P., and Cowtan, K. (2004) Coot: Model-building tools for molecular graphics. *Acta Crystallogr. D60*, 2126–2132.

(26) Schuettelkopf, A. W., and van Aalten, D. M. F. (2004) PRODRG: A Tool for High-Throughput Crystallography of Protein-Ligand Complexes. *Acta Crystallogr. D60*, 1355–1363.

(27) Laskowski, R. A., MacArthur, M. W., Moss, D. S., and Thornton, J. M. (1993) PROCHECK: A program to check the stereochemical quality of protein structures. *J. Appl. Crystallogr. 26*, 283–291.

(28) Ploeser, J. M., and Loring, H. S. (1949) The ultraviolet absorption spectra of the pyrimidine ribonucleosides and ribonucleotides. *J. Biol. Chem. 178*, 431–437.

(29) DeLano, W. L. (2002) *The PyMOL Molecular Graphics System*, DeLano Scientific, San Carlos, CA.

(30) Dontsova, M. V., Gabdoulkhakov, A. G., Molchan, O. K., Lashkov, A. A., Garber, M. B., Mironov, A. S., Zhukhlistova, N. E., Morgunova, E. Y., Voelter, W., Betzel, C., Zhang, Y., Ealick, S. E., and Mikhailov, A. M. (2005) Preliminary investigation of the three-dimensional structure of *Salmonella typhimurium* uridine phosphorylase in the crystalline state. *Acta Crystallogr. F61*, 337–340.

(31) Bennett, E. M., Li, C., Allan, P. W., Parker, W. B., and Ealick, S. E. (2003) Structural basis for substrate specificity of *Escherichia coli* purine nucleoside phosphorylase. *J. Biol. Chem. 278*, 47110–47118.

(32) Zhang, Y., Cottet, S. E., and Ealick, S. E. (2004) Structure of *Escherichia coli* AMP nucleosidase reveals similarity to nucleoside phosphorylases. *Structure 12*, 1383–1394.

(33) Lee, J. E., Cornell, K. A., Riscoe, M. K., and Howell, P. L. (2003) Structure of *Escherichia coli* 5′-methylthioadenosine/S-adenosylhomocysteine nucleosidase inhibitor complexes provide insight into the conformational changes required for substrate binding and catalysis. *J. Biol. Chem. 278*, 8761–8770.

(34) Ealick, S. E., Rule, S. A., Carter, D. C., Greenhough, T. J., Babu, Y. S., Cook, W. J., Habash, J., Helliwell, J. R., Stoeckler, J. D., and Parks, R. E., Jr. et al. (1990) et al. Three-dimensional structure of human erythrocytic purine nucleoside phosphorylase at 3.2 Å resolution. *J. Biol. Chem. 265*, 1812–1820.

(35) Kicska, G. A., Tyler, P. C., Evans, G. B., Furneaux, R. H., Kim, K., and Schramm, V. L. (2002) Transition state analogue inhibitors of purine nucleoside phosphorylase from *Plasmodium falciparum*. *J. Biol. Chem. 277*, 3219–3225.

(36) Krenitsky, T. A. (1976) Uridine phosphorylase from *Escherichia coli*. Kinetic properties and mechanism. *Biochim. Biophys. Acta 429*, 352–358.

(37) Thompson, J. D., Higgins, D. G., and Gibson, T. J. (1994) CLUSTAL W: Improving the sensitivity of progressive multiple sequence alignment through sequence weighting, position-specific gap penalties and weight matrix choice. *Nucleic Acids Res. 22*, 4673–4680.

(38) Pugmire, M. J., and Ealick, S. E. (1998) The crystal structure of pyrimidine nucleoside phosphorylase in a closed conformation. *Structure 6*, 1467–1479.